

Confocal Microscopy in Conjunction With Haemocytometry to Evaluate the Imperative Physical Characteristics of Multicellular Tumor Spheroids

Aziz UR RAHMAN (✉ aziz.rahman@uom.edu.pk)

University of Malakand

Research Article

Keywords: Interconversion of spheroid parameters, spheroid composition, compaction of spheroids, disaggregation of spheroids, confocal microscopy, haemocytometry

Posted Date: December 16th, 2021

DOI: <https://doi.org/10.21203/rs.3.rs-1107684/v1>

License:  This work is licensed under a Creative Commons Attribution 4.0 International License.

[Read Full License](#)

Abstract

Background: Tumor tissues resist penetration of therapeutic molecules. Multicellular tumor spheroids (MCTSs) were used as an *in vitro* tumor model. The aim of this study was to determine the growth of MCTSs with the age of spheroids, which could be applied and compared with *in vivo* drug uptake and penetration.

Method: Spheroids were generated by liquid overlay techniques, and their diameter was measured by confocal microscopy for up to two weeks. The trypan blue exclusion method was used to count dead and live cells separately via a hemocytometer.

Results: The pentaphysical characteristics of spheroids, including diameter, cell number, volume per cell, viability status, and estimated shell of viable and core of dead cells, were determined. The growth of spheroids was linear over the first week but declined in the 2nd week, which may be due to an overconcentration of dead cells and degraded products inside the spheroids, hence lowering the ratio of live cells in spheroids. Compaction of spheroids occurs from day 3 to day 7, with the mature spheroids having a low amount of extracellular space compared to intracellular volume.

Conclusion: Age-oriented growth of MCTSs provides a rationale to predict less rapid penetration as spheroids get older and could be correlated with *in vivo* tumors to predict pharmaceutical and therapeutic intervention.

1. Background

In vivo or *in vitro* exposure to carcinogens may transform normal animal cells into cancer cells [1]. HT-29 (a human colon adenocarcinoma cell line) possesses a good experimental system for the study of factors concerned with the differentiation of epithelial cells. The cytoskeleton adjusts accordingly as the cell changes its shape and environment or when it divides [2]. Multicellular tumor spheroids (MCTSs) imitate *in vitro* micrometastasis and the avascular stage of real tumor development, presenting a good situation to study tumor biology and to assess the effects of various therapeutic approaches [3–6]. The three-dimensional multicellular tumor spheroids (3-D MCTSs) acquire similarities with *in vivo* tumor tissues with respect to structural characterization. MCTSs have been used as an *in vitro* tumor tissue model to mimic *in vivo* tumor studies [7, 8]. Therefore, the selection of cell lines, proficiency in cell culture and spheroid generation are the core prerequisites for tumor tissue research. Penetration of drug molecules or cargo-drug conjugates varies from cell line to cell line [9–12], and selection of a particular cell line is essential according to the aims of biomedical research projects. Skills in cell culture and spheroid generation enhance insight into research outcomes. It has been reported that researchers must characterize and optimize the growth conditions for spheroid cells, which are selected for investigation [13]. While working with cancer cells, principles have been described, such as facilities in the lab, disposal methods, accessories and cell lines to work within the laboratory efficiently [14].

MCTSs have been proposed as a model of tumor tissue for experimental purposes. It exhibits similarities with tumor tissues in terms of composition, microenvironment and cellular behaviors [15, 16]. Development of such a technique that explores characteristic features of spheroids, such as the correlation of cell number with the age of spheroids, viability status of cells, extracellular volume per cell and distinct cellular layer in spheroids, could be a research-oriented therapeutic approach in the field of cancer research. To study spheroid composition and growth characteristics, we addressed spheroid geometry and explored many interesting observations/features for the characterization of spheroids. Changes in these features along with the age of spheroids can be correlated with the age of in vivo tumors, which can be used as a silent tool for cancer/tumor research.

2. Materials And Methods

2.1 Materials

2.1.1 Accessories for cell culture and spheroid generation

T-25 cm² and T-75 cm² cell culture flasks, 96-well plates, 15 ml centrifuge tubes were purchased from Corning (USA), Gilson pipettes of 20 µl, 200 µl, 500 µl and 1000 µl capacity (France made), multipipette (Swiss made), 20 ml Universal tubes, 10 ml pipettes (Barloworld Scientific Ltd, UK), light microscope (Olympus Optical Co Ltd, Japan) and Neubauer haemocytometer chamber.

2.1.2 Cell culture media and reagents

Dulbecco's modified Eagle's medium (DMEM), Dulbecco's modified Eagle's medium (DMEM) without phenol red, fetal bovine serum (FBS), L-glutamine, trypsin/EDTA were purchased from Invitrogen (UK), penicillin/streptomycin (P/S), phosphate-buffered saline (PBS) tablets, trypan blue solution (0.4% w/v), agarose powder and Accutase reagent were purchased from Sigma (UK), and Tat-FITC was purchased from Cambridge Bioscience (UK). The HT-29 cell line was kindly provided by a laboratory colleague in the drug delivery group at Manchester Pharmacy School, The University of Manchester (UK).

2.2 Methods

2.2.1 Monolayer Cell Culture in Two-Dimension (2-D)

The HT-29 cell line was grown in T-75 cm² cell culture flasks and kept in an incubator maintained at 37°C in a humidified atmosphere and 5% CO₂. The culture medium was changed on alternate day. When the cell confluence reached approximately 70%, cells were detached from the flasks using either trypsin/EDTA or Accutase.

2.2.2 Generation of 3-D Multicellular Tumor Spheroid (3-D MCTS)

Spheroids were generated by the liquid overlay technique [17]. According to this technique, approximately 200 μ l of cell suspension containing 2000 cells/well (HT-29 cell line) was transferred to each well of a 96-well agarose gel-coated plate. The cell suspension was composed of cell culture media (DMEM containing 4.5 g/l glucose) supplemented with 10% FBS (fetal bovine serum) and 1% (v/v) penicillin/streptomycin (P/S) and L-glutamine. The seeded 96-well plates were kept in an incubator maintained at 37°C, a humidified atmosphere and 5% CO₂ for 3 days (72 hrs.). After a three-day incubation period, all wells of 96-well plates were checked for the formation and shape of spheroids. Observations regarding the shape and size of spheroids were recorded. A sample of spheroid has been depicted in Figure 1(a). Only those spheroids were selected for experimental observations that were of spherical shape and the same size after three days of spheroid generation and retained the same characteristics until the day of observation/experiment.

2.2.3 Disaggregation of spheroids

Five spheroids per day were selected for each disaggregating treatment, either through accutase or trypsin/EDTA. Each spheroid was disaggregated by Accutase or 0.5x trypsin/EDTA (T/E). Then, 100 μ l of disaggregating reagents was added to each spheroid for disaggregation. Then, a sufficient volume of PBS (2.9 ml) was added to make up the cell suspension up to 3 ml of each spheroid and pipetted well to form a uniform suspension. Then, 20 μ l from these suspensions was mounted on a hemocytometer, and the number of cells in each spheroid was counted.

2.2.4 Calculating the viable and dead cells in spheroids after disaggregation

After disaggregation of spheroids, the viability test of each spheroid was performed by staining with trypan blue solution (0.4%). Dead cells were stained with trypan blue solution, while viable cells remained unstained. Then, the numbers of viable and dead cells were counted separately through a hemocytometer.

2.2.5 Calculating the number of cells in a spheroid from its diameter (through mathematical calculation)

To estimate the number of cells in a spheroid from its diameter, spheroids were washed with phosphate-buffered saline (PBS) and transferred from a 96-well culture plate to an 8-well plate along with one drop of PBS. Then, one side of the spheroid was mechanically dissociated with the tip of the pipette inside the 8-well plate, as shown in Figure 1(b). Then, we imaged the spheroids with confocal microscopy in DIC (differential interference contrast) mode. The mean diameter of these disaggregated cells is essential for the interconversion of spheroid parameters. These parameters include the number of cells in the spheroid, diameter of the spheroid, volume of the spheroid, cellular layer in a spheroid and estimation of dead cell and viable cell regions.

For this purpose, the diameter of 20 disaggregated cells, as mentioned in the encircled area of Figure 2, was measured through confocal software, and the mean diameter was calculated. The calculated mean

diameter (d) of a single cell was approx.: 15 μm . The volume of a single cell (v) was also calculated by the formula $v = 4/3\pi r^3$ (where r is radius of a single cell), which was approximately equal to 1800 μm^3 .

The conversion of spheroid parameters was calculated by the following formulas:

From diameter to spheroid volume and from volume to number of cells (without haemocytometry)

Radius was calculated from the diameter of the spheroid ($R=D/2$), where R is the radius and D is the diameter.

To calculate volume of a spheroid (V); $V= 4/3\pi R^3$

To calculate number of cells from volume of spheroid

Number of cells = Volume of spheroid/volume of a single cell

From number of cells to spheroid diameter (using haemocytometry):

From the number of cells, the volume of spheroid is calculated by the formula:

$V= \text{single cell volume} \times \text{number of cells in a spheroid}$

To estimate the diameter of the spheroid from its volume, the following formula was used:

$$D = (6 V/\pi)^{1/3}$$

Similar equations were applied to estimate the number of cells, volume and diameter in dead cell and viable cell regions.

The diameter and volume of a single cell is essential for the interconversion of spheroid parameters. Therefore, it was calculated after disaggregation of cells from a spheroid. It should be noted that the HT-29 cell monolayer, when attached to the glass surface, shows a higher diameter (18 μm) than the diameter obtained from disaggregated spheroid cells (15 μm). The reason for this variation in diameter is that HT-29 cells attached to the glass surface may attain a flat shape, while cells after disaggregation from spheroids are rounded in shape. Therefore, the diameter of freshly disaggregated cells was considered for calculation.

2.2.6 Calculating the approximate layers of cells in spheroids

The approximate layers of cells in spheroids, dead cells and viable cell regions were estimated by the formula:

Layers of cells = Thickness of spheroid or thickness of a particular region divided by a single cell diameter

2.2.7 Interconversion of spheroids parameters

For interconversion of spheroid parameters, the diameter and volume of a single cell is mandatory. Therefore, the HT-29 single-cell diameter was measured, which was approx. 15 μm . Then, the volume of a single cell was calculated from the diameter, which was approximately equal to 1800 μm^3 . The diameter of spheroids was measured through confocal microscopy, while the total cell number and viability status of each spheroid were determined through haemocytometry. Afterwards, through interconversion of spheroid parameters, the diameter, volume per cell, number of cells in dead and viable cell regions of each spheroid and radii (radii of spheroids, shell of live and core of dead cell regions) were calculated.

3. Results

3.1 Spheroid's geometry

From Figure 2, in the larger spheroids (spheroids number 1 and 2), the cell count is lower than might be expected, as indicated by a much higher volume per cell. Larger spheroids develop a central necrotic region and a hypoxic region [18]. Therefore, well-established hypoxic and necrotic regions might exist in more mature spheroids, day 7 and onward. The larger spheroids could also indicate that spheroids become unstable and necrotic after exceeding a diameter of 800 microns.

For the two smaller spheroids (spheroids 3 and 4), the volume per cell is very close to what we estimated as the intracellular volume (estimated from images of single disaggregated cells). This suggests that the spheroids (by this age and provided they do not get too big and necrotic) consist of very tightly packed cells with a small (~10% or less) extracellular volume fraction like many tissues. When comparing spheroids with tumor tissue, it should be noted that the cell packing is similar, but the synthesis of extracellular matrix (ECM) proteins might not be similar. It has been reported that in vivo ECM is mostly produced from host stromal cells and that in spheroids, it is produced from tumor cells. This difference causes variation in the gene-producing constituents of the ECM [8]. The outermost shell of viable cells is very thin, with only a few cells thick for all spheroids. This may be explained by technical problems with trypan blue staining, as it led to underestimation of the viable fraction. As trypan blue interacts with serum protein [19], it may overestimate the dead cells and hence underestimate the viable fraction of cells when using trypan blue exclusion techniques.

3.2 Diameter versus age of spheroids

Spheroid diameter (determined by confocal microscopy of intact spheroids) has not yet faced the subsequent disaggregation treatment, so these measurements can be taken as primary controls for subsequent measurements. The diameter of spheroids versus age is depicted in Figure 3. The growth curve shows that the tumor mass does not grow at an exponential or even linear rate. Growth appeared linear over the first week after seeding, but after day 9, the growth rate appeared to decrease and form a plateau, and there appeared to be greater variability in spheroid size.

3.3 Cell number versus age of spheroids

These measurements were supposed to be affected by the spheroid disaggregation method used. Therefore, the data were split according to the enzymatic treatment (accutase versus trypsin/EDTA). The analyses show that the effect with respect to spheroid age is highly significant (ANOVA, $p < 0.01$), but the comparison of disaggregation methods was statistically nonsignificant (ANOVA, $p > 0.05$). The cell number of spheroids versus age is shown in Figure 4. The growth of cells (in terms of cell number) appeared linear over the first week after seeding, but the rate (cell number per day) appeared to decline after 9 days. It is also evident that the Accutase disaggregation method appears to yield higher cell counts, particularly in the more mature spheroids. The possible reason may be that dead or dying cells seem to be more sensitive to trypsin/EDTA than accutase treatment. Therefore, more cells were obtained by accutase treatment than trypsin/EDTA treatment.

3.4 Volume per cell versus age of Spheroids

After diameter measurement through confocal microscopy, the spheroids were subjected to disaggregation through Accutase reagent or trypsin/EDTA. The volume per cell obtained is shown in Figure 5. The difference in volume/cell obtained with Accutase reagent versus trypsin/EDTA was statistically nonsignificant (ANOVA, $p > 0.05$). The volume per cell via accutase treatment is more realistic and has comparative similarity with theoretical calculations in terms of volume per cell, most particularly on the 7th day of spheroid age (spheroid compaction stage). Therefore, we prefer accutase treatment to trypsin/EDTA treatment as a spheroid disaggregating reagent. Observations by confocal microscopy led to the calculation that the diameter of a single HT-29 cell was $15 \mu\text{m}$, which corresponds to a volume of $1,800 \mu\text{m}^3$ if the cell is assumed to be a sphere. Within the spheroid, there will be an additional extracellular volume associated with each cell. One approach is to combine spheroid volume and estimated cell number to explore the volume per cell within the spheroid, excluding the trypsin-treated group for reasons discussed previously.

3.5 Cells viability versus age of spheroids

The viability measurement was performed by trypan blue staining. The cell viability decreased with the age of the spheroids, as shown in Figure 6. Variations in the viable fraction as a function of spheroid age and disaggregation method were noted. However, as noted previously, the effect of the disaggregation method was not statistically significant (ANOVA, $P > 0.05$).

3.6 Thickness of distinct cell regions versus age of spheroids

Cellular layers of distinct cell regions, such as radii of spheroids, core of dead cell regions or thickness (shell) of live cell regions, were estimated and are shown in Figure 7. The presented data could be applied to a simple model of spheroid structure, in which a core of nonviable cells is covered with a shell of viable cells.

3.7 Cellular layers of distinct cell regions versus age of spheroids

The analysis suggests that the outer layer of viable cells grows during the first week, as shown in Figure 8, but by day 7, it stabilizes at a maximum value of approximately 80 μm (~5 cell diameters). On the other hand, the nonviable core continues to grow during the second week, albeit at a slower rate.

4. Discussion

The ratio of live and dead cells as well as the diameter of the necrotic region in a spheroid is an important issue for the delivery and penetration of molecules. Necrosis might be due to insufficient in- and out-flow of oxygen, nutrients and other negative positive regulators [7, 20]. Penetration in all live cells is the most efficient and advantageous, but there is no simple method to estimate the ratio of live and dead cells and to estimate the necrotic region. Therefore, we presume that this method could cover the gap and could estimate the various parameters of spheroids. This is a simple method for estimating the diameter, number of cells, volume per cell, thickness of distinct regions and cellular layers in spheroids. The possible reason for spheroid diameter variability may be due to an increase in spheroid age, and the accumulation and concentration of dead cells increases in the inner region. This results in an increase in waste products and their flow across the spheroid, which might affect the growth rate. The cell number along the age of spheroids indicates that accutase treatment leads to a greater degree of disaggregation into single cells and hence a higher and more accurate estimate of the total number of cells in the spheroid. The haemocytometry results from the accutase group were more reliable than trypsin/EDTA treatment because we obtained a greater number of cells in mature spheroids with former than latter. Therefore, in subsequent experimental procedures, accutase treatment was used exclusively.

The volume per cell analysis appears to show dependence on spheroid age. This observation could be explained based on the three-stage process of spheroid growth, comprising an initial loose form followed by a packing/compaction process during spheroid formation, followed by the development of a hollow necrotic core in the larger more mature spheroids. Here, it should be noted that we assumed that the volume of dead and necrotic cells equals that of live cells. In actual cases, the volume of dead cells may be quite lower than that of live cells. Moreover, necrotic region estimation is also based on the volume difference of the actual cell volume and the calculated cell volume. Therefore, taking into consideration the effect of dead cell volume and necrotic region volume, the volume per cell along the age of spheroids may increase and lead to the development of a necrotic core in larger more mature spheroids. There was initially a loose packing of cells, but as time progressed, the volume per cell approached $1500 \mu\text{m}^3$, meaning that cells were tightly packed and extracellular volume was negligible in the live cell region, as evident from day 7 onward. Additionally, there was development of a well-established necrotic region from day 7 onward, which justified that the age of spheroids could play a role in the penetration of molecules. Therefore, it addresses the objectives that spheroid geometry/distinct cellular distribution changes with the passage of time and could alter penetration of drug/fluorophore(s) in spheroids.

As far as the viability of cells along the age of spheroids is concerned, the effect of spheroid age shows that there is a small but significant reduction in the viable cell fraction after the first week of growth. This reduction in the viable cell fraction might be due to the accumulation of dead cells and degraded products that affect the growth of viable cells. On the other hand, the fraction of dead cells increased at day 9 and then stabilized.

Regarding the thickness of distinct regions in spheroids with age, it has been reported that larger spheroids develop a central necrotic region and a hypoxic region [18]. Therefore, well-established hypoxic and necrotic regions might exist in more mature spheroids, day 7 and onward. Trypan blue also interacts with proteins [19]; therefore, the dead cell count might be overestimated. At an early age (day 3 particularly & day 5), cell-cell contact in spheroids may be loose, leading to compaction. Moreover, at these early age spheroids, distinct cells may be mixed with each other, and the hypoxic region may not be well established. On day 7 and onward, a well-established hypoxic region and necrotic region might take place. The results of the model are illustrated above, which represent the estimated radii of spheroids, estimated radii (core) of the dead cell region and estimated thickness (shell) of the live cell region. The cellular layers suggest that necrotic and hypoxic regions in larger spheroids [18] increase with the age of spheroids, while the viable cell layer decreases.

5. Conclusion

The growth curve may vary from one cell line to another cell line due to its inherent characteristics. The growth of spheroids (HT-29) has been divided into three phases: the loose aggregate form, compact form without developed necrotic region and compact form with a developed necrotic region. From day 7 to day 11, the diameter of spheroids ranged from 550-650 μm . At this interval, the spheroids will be in a compact form and will possess three distinct regions: a well-developed proliferating region, a hypoxic region, and a necrotic region. It is presumed to be the appropriate duration to use spheroids as tumor tissue models for experimental/anticancer drug delivery purposes. The results and analysis of spheroid geometry revealed that spheroid geometry changes as it gets older and meets the objectives that spheroid geometry/distinct cellular distribution changes with the passage of time, and it could alter penetration of drug/fluorophore(s) in spheroids.

Abbreviations

MCTSs (Multicellular Tumor Spheroids); CLSM (Confocal Laser Scanning Microscope); DIC (Differential Interference Contrast); HT-29 (Human Adenocarcinoma Colorectal cell line); ANOVA (Analysis of Variance).

Declarations

Ethics approval and consent to participate:

Not applicable

Consent for publication:

The journal is authorized to publish the manuscript after acceptance.

Availability of data and material:

It will be provided as and when requested by the publisher.

Competing interests:

The author declares no conflict of interest.

Funding:

This research study was financially supported by the Higher Education Commission (HEC) Pakistan, through University of Malakand, and Manchester Pharmacy School, The University of Manchester, UK.

Authors' contributions:

All work was conducted by a single author.

Acknowledgements:

The author is thankful to Dr. David Berk and Dr. Alain Pluen for their guidance and cooperation during the research study in Manchester Pharmacy School, The University of Manchester, UK.

References

1. Stiles, C.D., et al., *Relationship of cell growth behavior in vitro to tumorigenicity in athymic nude mice*. Cancer Res, 1976. **36**(9 pt.1): p. 3300-5.
2. Cohen, E., I. Ophir, and Y.B. Shaul, *Induced differentiation in HT29, a human colon adenocarcinoma cell line*. J Cell Sci, 1999. **112 (Pt 16)**: p. 2657-66.
3. Guirado, D., et al., *Dose dependence of the growth rate of multicellular tumour spheroids after irradiation*. Br J Radiol, 2003. **76**(902): p. 109-16.
4. Virgone-Carlotta, A., et al., *In-depth phenotypic characterization of multicellular tumor spheroids: Effects of 5-Fluorouracil*. PLoS One, 2017. **12**(11): p. e0188100.
5. LaBarbera, D.V., B.G. Reid, and B.H. Yoo, *The multicellular tumor spheroid model for high-throughput cancer drug discovery*. Expert Opin Drug Discov, 2012. **7**(9): p. 819-30.
6. Sant, S. and P.A. Johnston, *The production of 3D tumor spheroids for cancer drug discovery*. Drug Discov Today Technol, 2017. **23**: p. 27-36.

7. Kunz-Schughart, L.A., *Multicellular tumor spheroids: intermediates between monolayer culture and in vivo tumor*. Cell Biology International, 1999. **23**(3): p. 157-161.
8. Kim, J.B., *Three-dimensional tissue culture models in cancer biology*. Seminars in Cancer Biology, 2005. **15**(5): p. 365-377.
9. Mann, D. and A. Frankel, *Endocytosis and targeting of exogenous HIV-1 Tat protein*. The EMBO Journal, 1991. **10**(7): p. 1733-1739.
10. Hällbrink, M., et al., *Cargo delivery kinetics of cell-penetrating peptides*. Biochimica et Biophysica Acta (BBA) - Biomembranes, 2001. **1515**(2): p. 101-109.
11. Mai, J.C., et al., *Efficiency of Protein Transduction Is Cell Type-dependent and Is Enhanced by Dextran Sulfate*. J. Biol. Chem., 2002. **277**(33): p. 30208-30218.
12. Tunnemann, G., et al., *Cargo-dependent mode of uptake and bioavailability of TAT-containing proteins and peptides in living cells*. FASEB J., 2006. **20**(11): p. 1775-1784.
13. Sutherland, R.M. and R.E. Durand, *Growth and cellular characteristics of multicell spheroids*. Recent Results Cancer Res, 1984. **95**: p. 24-49.
14. Cree, I.A., *Principles of cancer cell culture*. Methods Mol Biol, 2011. **731**: p. 13-26.
15. Kostarelos, K., et al., *Binding and interstitial penetration of liposomes within avascular tumor spheroids*. International Journal of Cancer, 2004. **112**(4): p. 713-721.
16. Kostarelos, K., et al., *Engineering lipid vesicles of enhanced intratumoral transport capabilities: correlating liposome characteristics with penetration into human prostate tumor spheroids*. J Liposome Res. , 2005. **15**(1-2): p. 15-27.
17. Carlsson, J., et al., *Formation and growth of multicellular spheroids of human origin*. Int. J. Cancer 1983. **31**: p. 523-533.
18. Minchinton, A.I. and I.F. Tannock, *Drug penetration in solid tumours*. Nat Rev Cancer, 2006. **6**(8): p. 583-592.
19. Gao, H.-W. and J.-F. Zhao, *Interaction of Trypan Blue with Protein and Application*. Journal of the Chinese Chemical Society, 2003. **50**(2): p. 329-334.
20. Durand, R.E. and R.M. Sutherland, *Dependence of the Radiation Response of an in Vitro Tumor Model on Cell Cycle Effects*. Cancer Res, 1973. **33**(2): p. 213-219.

Figures

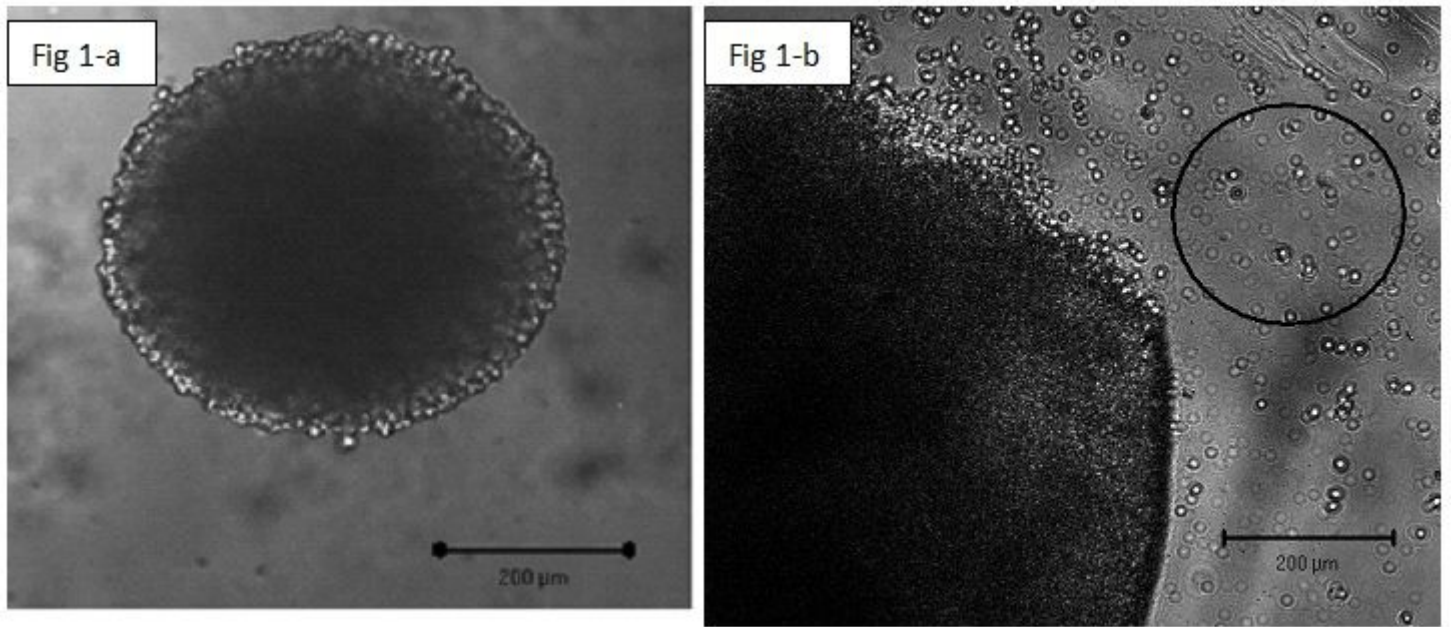


Figure 1

(a) DIC image of 5-day-old spheroids obtained through confocal microscopy. The spheroids were generated by liquid overlay techniques [17] in a 1.5% agarose-coated 96-well plate. Approximately 2000 cells/200 μl of culture media were seeded in 96-well plates containing DMEM supplemented with 10% FBS and one percent penicillin/streptomycin & L-glutamine. The plates were kept in an incubator at 37 °C, supplemented with 5% CO₂ and a humidified atmosphere for three days. The images of spheroids were taken in DIC (differential interference contrast) mode. The microscope objective setting was 10x/0.3. Scale bar represents 200 μm. **(b) Mechanical disaggregation of a side of spheroid.** The spheroid was kept in an 8-well plate with one drop of PBS. One side of the spheroid was mechanically disaggregated through the tip of a pipette. The spheroids were observed under a confocal microscope in DIC mode. The diameter of freshly disaggregated individual cells was then measured. The microscope objective setting was 10x/0.3. Scale bar represents 200 μm.

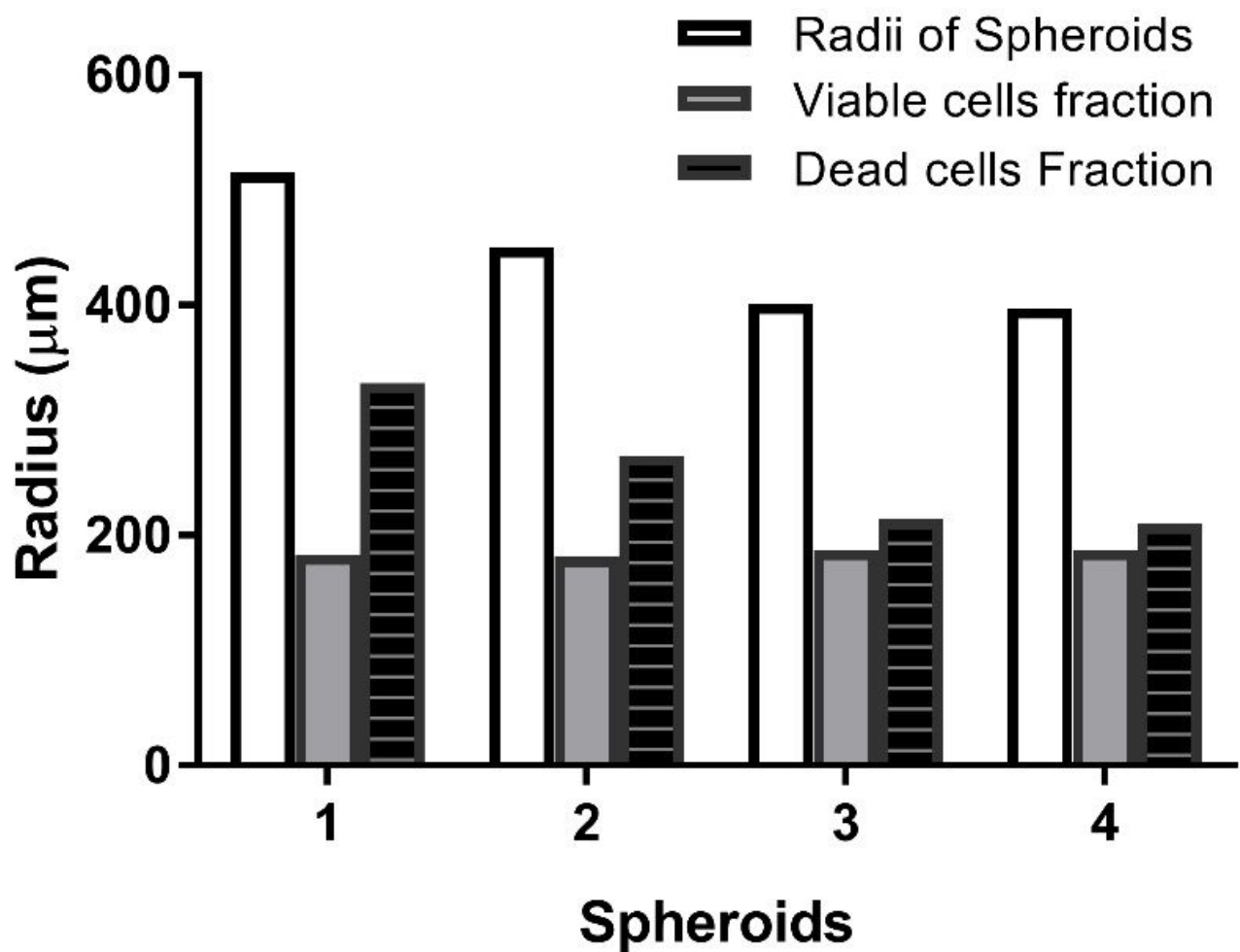


Figure 2

Spheroid geometry based on haemocytometry. Diameters of 16-day-old HT-29 tumor spheroids were taken through confocal microscopy in DIC mode. The microscope objective setting used was 10x/0.3. The results showed that the necrotic region increased with age as well as with the size of spheroids. Four spheroids were taken for observations; numeric 1-4 represents the respective spheroids.

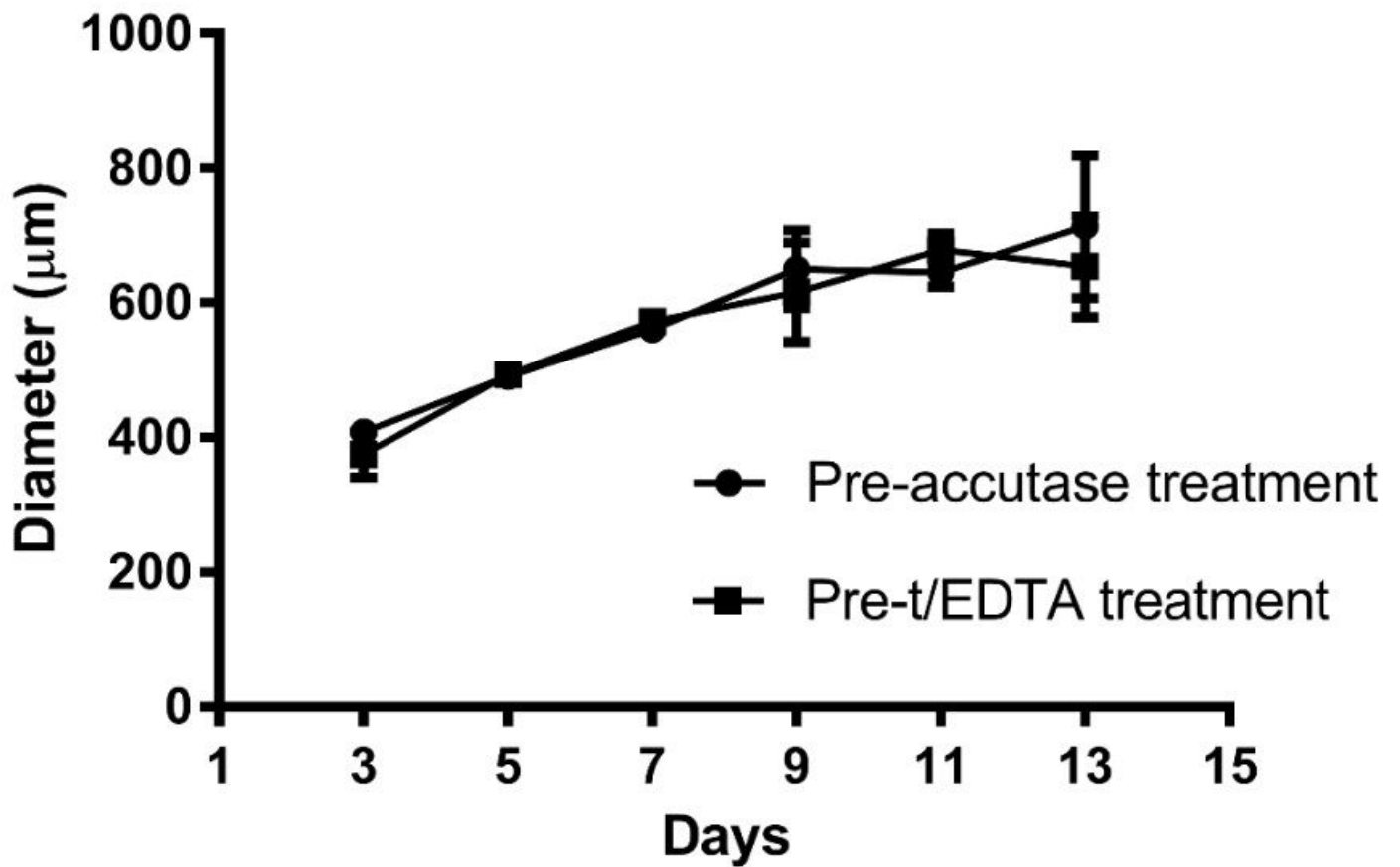


Figure 3

Diameter versus age of spheroids. The diameter of spheroids was measured by confocal microscopy in DIC mode. The microscope objective setting was 10x/0.3. The diameter of spheroids was found to increase from day 3 to 7 in a linear shape and form a plateau shape from days 9- 13. A total of 5 spheroids were taken for each observation. Each value is the mean \pm SD, n=5

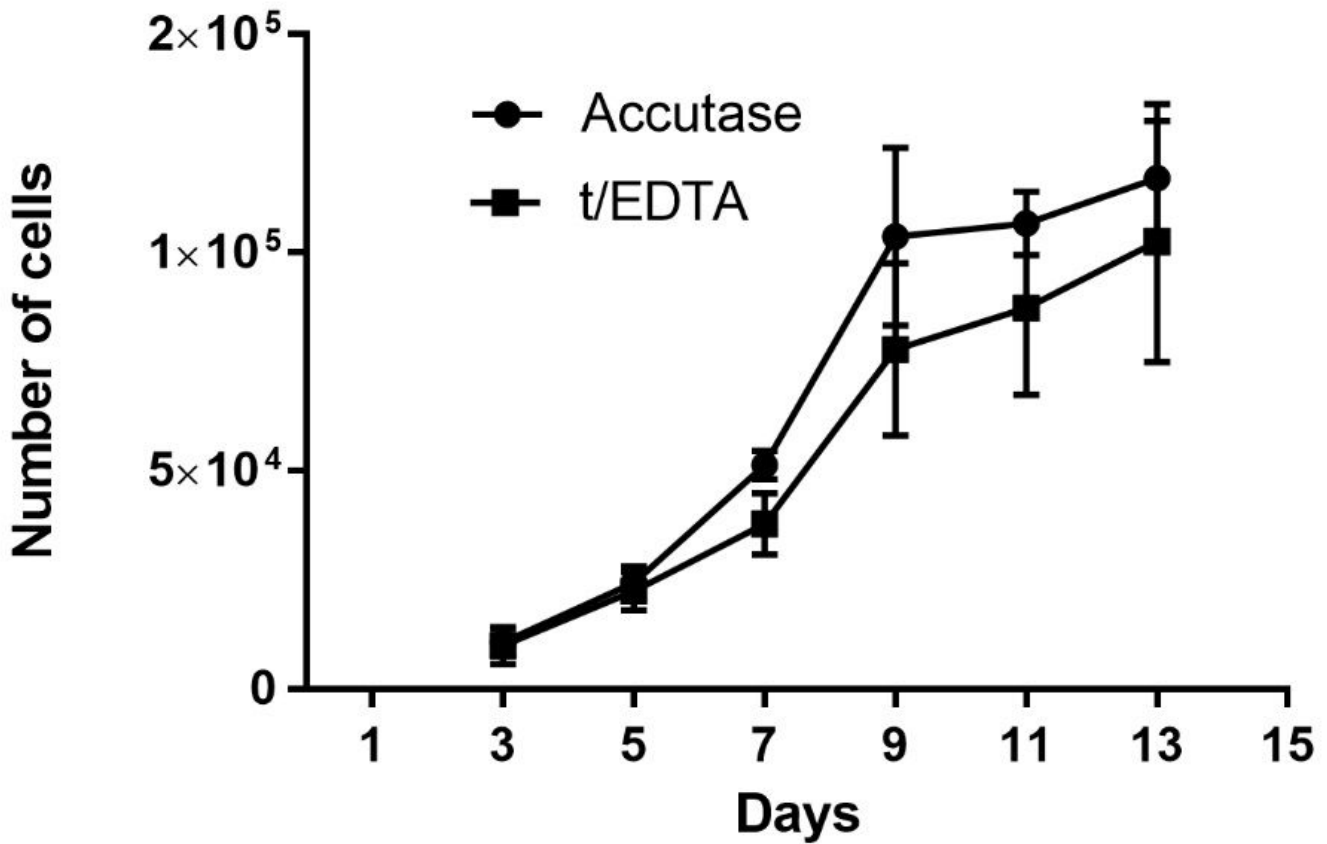


Figure 4

Cell number versus age of spheroids. The cell number in spheroids was counted through a hemocytometer after disaggregation treatment. The effect of increasing cell number with respect to days was statistically significant (ANOVA, $p < 0.01$). The Accutase disaggregation method appeared to yield higher cell counts, particularly in the more mature spheroids, than the trypsin disaggregation method, but the difference was statistically nonsignificant (ANOVA, $p > 0.05$). Each value is the mean \pm SD, $n = 5$.

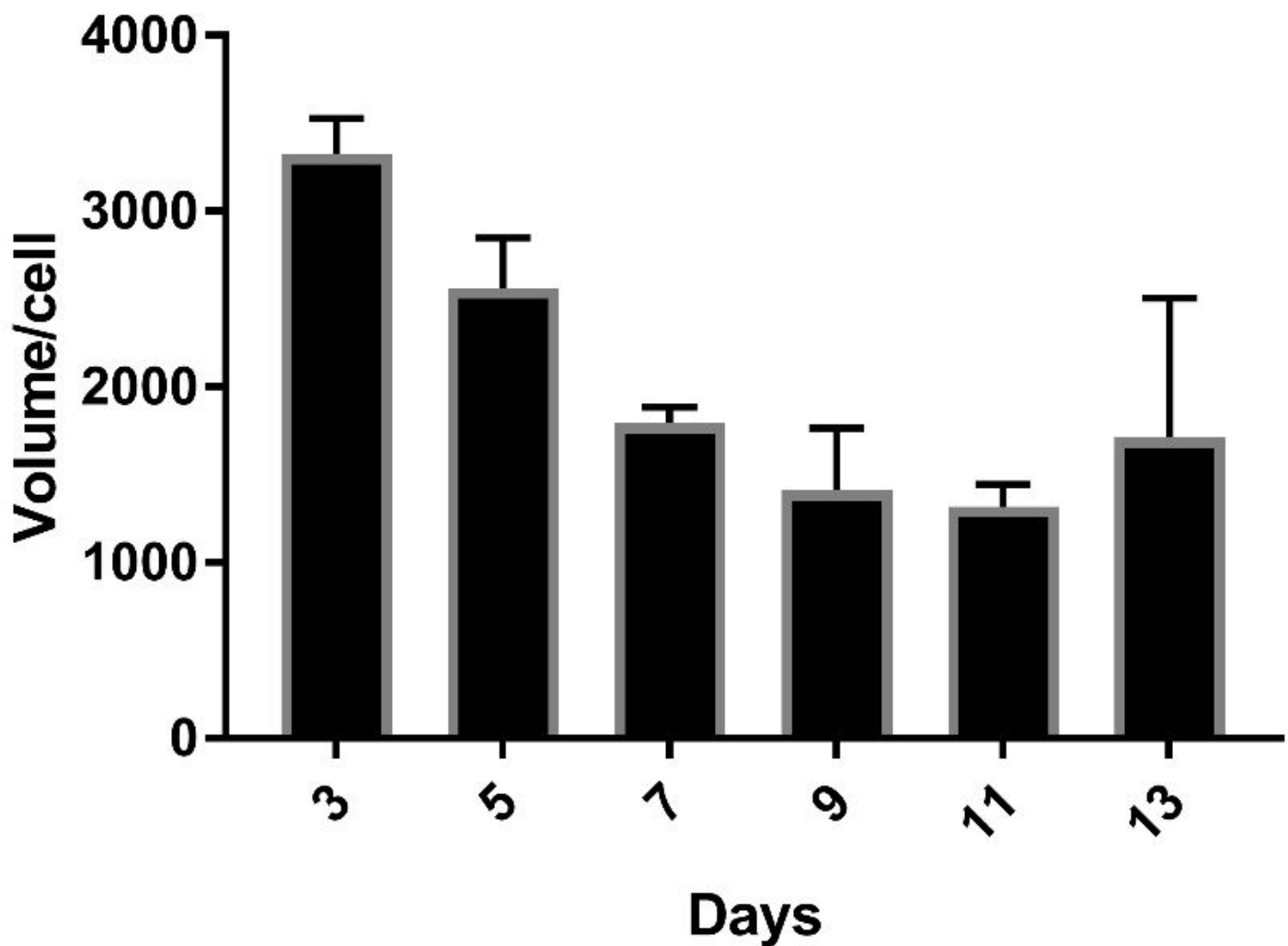


Figure 5

Volume per cell versus age of spheroids. The volume per cell was obtained by dividing the volume of spheroids by the total number of cells in the respective spheroids. The volume per cell decreases with the age of spheroids, reaching up to a single cell volume on day 7, as theoretically calculated ($1,800 \mu\text{m}^3$), while a further decrease in extracellular volume may represent the accumulation of degraded products of cells and the development of necrotic regions. Moreover, there may be initially a loose packing of cells, but as time progresses, the volume per cell approaches $1500 \mu\text{m}^3$, meaning that the cells are tightly packed, and the extracellular volume is negligible. A total of 5 spheroids were taken for each observation. Each value is the mean \pm SD, $n = 5$.

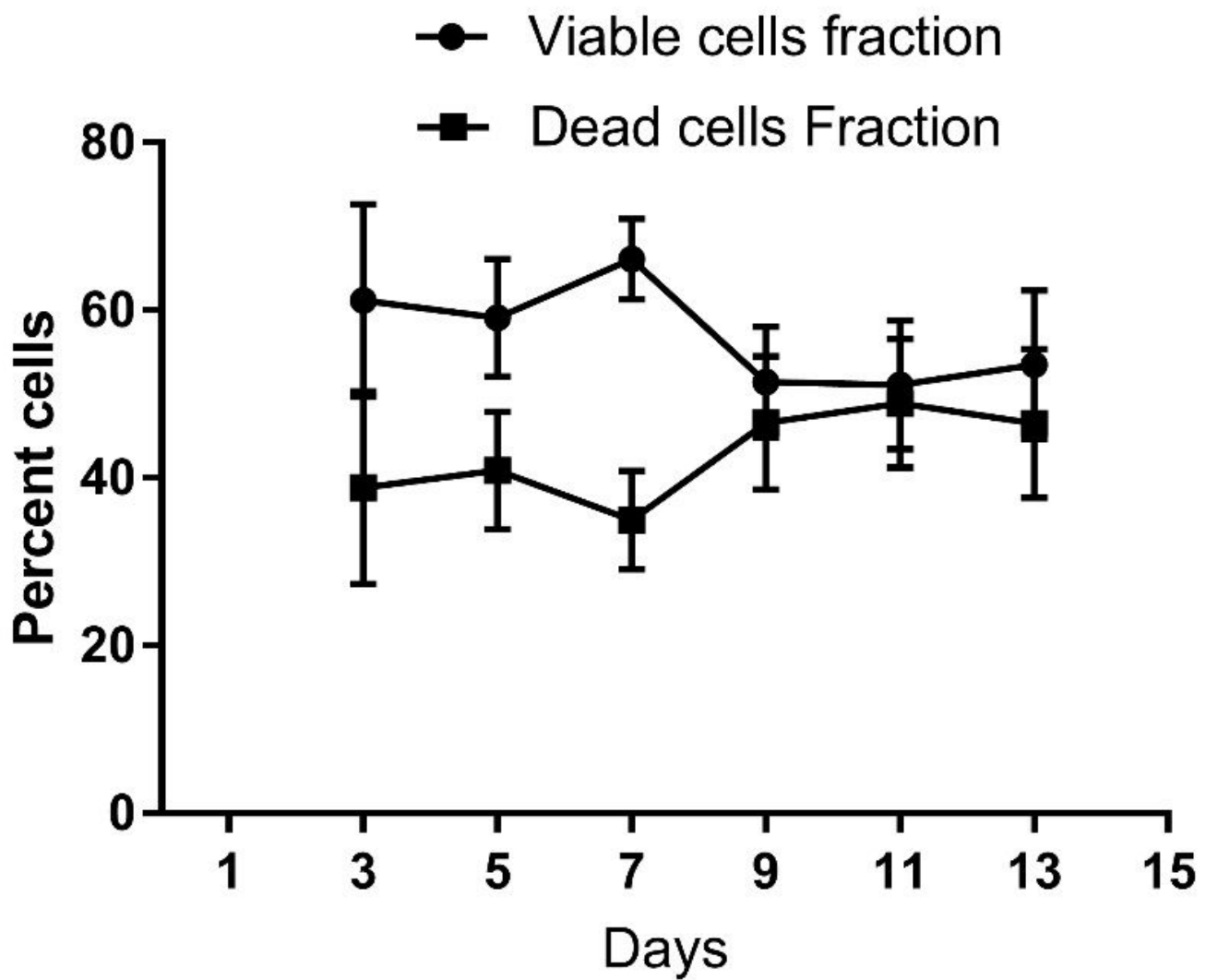


Figure 6

Dead and viable cell fractions versus age of spheroids. The viability status was determined by trypan blue staining. Dead cells were stained with trypan blue, while live cells remained unstained. The percentage of live cells was between 50 and 70%, while that of dead cells was between 30 and 50%. It shows the accumulation of dead cells and degraded products with the age of spheroids, which affects the percentage of viable cells. Each value is the mean \pm SD, n = 10 (in the case of 15-day-old spheroids, n = 5).

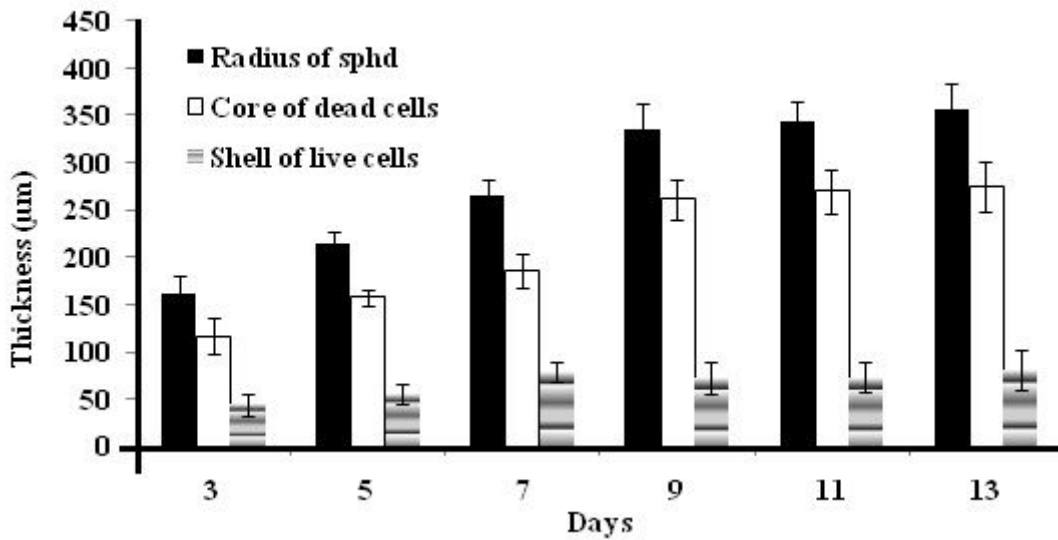


Figure 7

Thickness of distinct regions along with the age of spheroids. The radii of spheroids starting from 150 µm reach 340 µm on the 9th day and then stabilize. The core of the dead cell region increases from 110 µm, reaches 260 µm at 9 days and then stabilizes. The thickness of the live cell region (shell) starting from 45 µm thickness reached 80 µm thickness on the 7th day and then stabilized. This suggests that spheroids rapidly grow up to a certain time beyond which their growth stabilizes. Each value is the mean \pm SD, n = 10

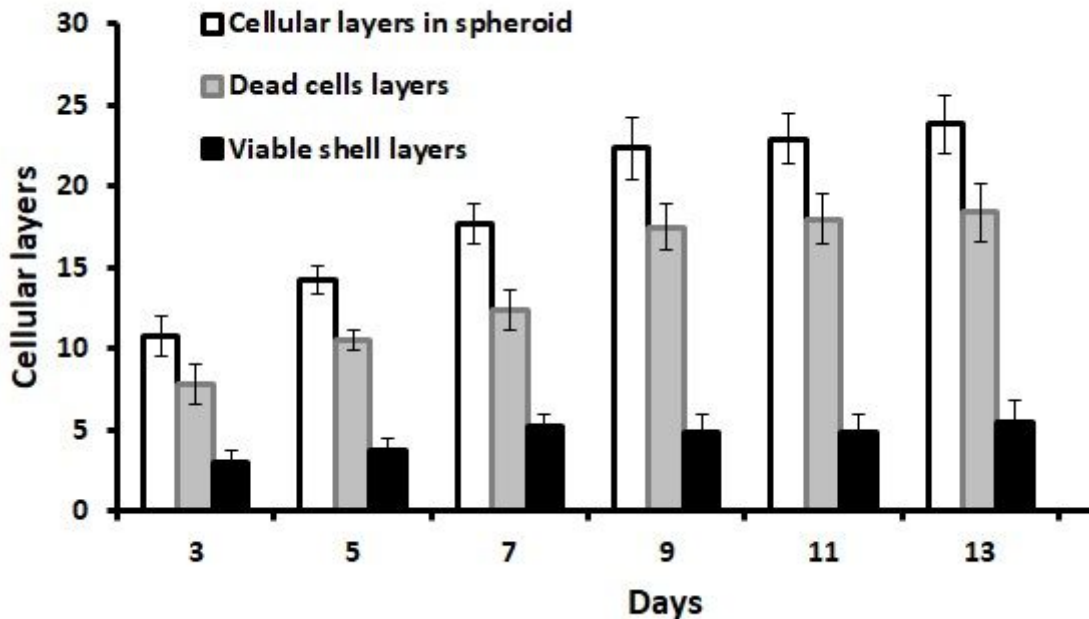


Figure 8

Cellular layers of distinct regions along with the age of spheroids. The shell of the viable cell layer starting from day 3 reached 5 on the 7th day and then stabilized. The number of dead cell layers increased from 8 to 17 on the 9th day and then stabilized. The cellular layers of spheroids starting from 11 on day 3 reached 23 on the 9th day and then stabilized. This suggests that spheroids rapidly grow up to a certain time beyond which their growth stabilizes. Each value is the mean \pm SD, n = 10